Al-Mustaqbal Journal of Pharmaceutical and Medical Sciences

Volume 2 | Issue 1 Article 1

2024

Development of a Multi-Target Pharmacophore-Based Virtual Screening Agent Against COVID-19

Nashwa A. Ibrahim
Medicinal chemistry department, Faculty of Pharmacy, Beni-Suef University, Beni-Suef 62514, Egypt,
nashwa.ahmed@pharm.bsu.edu.eg

Ahmed M. Gouda
Medicinal chemistry department, Faculty of Pharmacy, Beni-Suef University, Beni-Suef 62514, Egypt,
ahmed5_pharm5@yahoo.com

Hany A. M. El-Sherief
Department of Pharmaceutical Chemistry, Faculty of Pharmacy, Deraya University, Minia, Egypt,
hany.abdeltawab@deraya.edu.eg

ISSN: 2959-8974 – e-ISSN: 3006-5909

Recommended Citation

Ibrahim, Nashwa A.; Gouda, Ahmed M.; and El-Sherief, Hany A. M. (2024) "Development of a Multi-Target Pharmacophore-Based Virtual Screening Agent Against COVID-19," *Al-Mustaqbal Journal of Pharmaceutical and Medical Sciences*: Vol. 2 : Iss. 1 , Article 1.
Available at: https://doi.org/10.62846/3006-5909.1005

ORIGINAL STUDY

Development of a Multi-Target Pharmacophore-Based Virtual Screening Agent Against COVID-19

Nashwa A. Ibrahim [a], Ahmed M. Gouda [a], Hany A. M. El-Sherief [b,*]

[a] Medicinal chemistry department, Faculty of Pharmacy, Beni-Suef University, Beni-Suef 62514, Egypt
[b] Department of Pharmaceutical Chemistry, Faculty of Pharmacy, Deraya University, Minia, Egypt

ABSTRACT

The worldwide outbreak of the COVID-19 pandemic compelled scientists to develop new, highly effective therapeutic approaches to fight it. Multitarget drugs have been proven to be effective in managing complex disorders. But designing multitarget drugs is a great challenge. In this study, to prevent a lack of efficacy due to viral mutation escape, a multi-target agent against the COVID-19 virus was discovered. As crucial targets, RNA-dependent RNA polymerase (RdRp), COVID-19 main protease (Mpro), and SARS-CoV-2 Nsp15 were selected. A pharmacophore model was developed using the native ligands of the chosen targets. This model was used to screen the ZINC Drug Database for commercially available compounds having similar features to the experimentally tested drugs. Pharmacophore-based virtual screening yielded 1331 hits, which were further docked into the binding sites of selected proteins using PyRx AutoDock Vina. Evaluation of docking results revealed that glisoxepide (Zn 00537804) has the highest binding scores for the three target proteins. It showed binding free energies of −6.8, −6.2, and −7.8 kcal/mol towards SARS-CoV-2 Mpro, Nsp15, and RdRp, respectively. According to an *in silico* ADME study, glisoxepide follows Lipinski's rule. The results of a molecular dynamics simulation study and subsequent investigations showed that glisoxepide had good dynamics and stability within the active sites of selected targets. The promise of glisoxepide as a potential treatment for SARS-CoV-2 still needs to be further evaluated through experimental research.

Keywords: Multi-target pharmacophore, Virtual screening, Anti-SARS-CoV-2 RdRp, Mpro, and Nsp15, Molecular docking, Molecular dynamics simulation, Glisoxepide

1. Introduction

In December 2019, the severe acute respiratory syndrome-related coronavirus 2 (SARS-CoV-2, COVID-19) attacked the world, and the respiratory sickness spread quickly [1]. In March 2020, the World Health Organization (WHO) declared the infection a pandemic disease due to its rapid spread in 225 countries, which resulted in 774,771,942 confirmed cases of COVID-19 and 7,035,337 fatalities as of 25th February 2024, 13.59 billion doses of the vaccine had been administered (https://covid19.who.int/) [2]. The Coronaviridae family includes the SARS-CoV-2 virus. It is an enveloped (+ss) RNA betacoronavirus whose genomes encode several accessory proteins, structural proteins, and non-structural proteins (nsps) [3]. Most people have a moderate infection, but the elderly or those who have underlying medical conditions, including cancer, diabetes, cardiovascular disease, or chronic respiratory disease, are more likely to experience a serious sickness that can lead to pneumonia, respiratory distress, and organ damage [4]. Most nations throughout the world have implemented extremely limited safety measures that are insufficient to stop the COVID-19 virus waves from spreading. The situation has improved with recently

Received 25 January 2024; accepted 22 March 2024.
Available online 30 May 2024

* Corresponding author.
E-mail addresses: nashwa.ahmed@pharm.bsu.edu.eg (N. A. Ibrahim), ahmed5_pharm5@yahoo.com (A. M. Gouda), hany.abdeltawab@deraya.edu.eg (H. A. M. El-Sherief).

https://doi.org/10.62846/3006-5909.1005

licenced vaccines, but returning to normal conditions is still challenging, and infections are still increasing, especially considering the emergence of new virus strains that may be more resistant to vaccines. These variations emerged because of modifications to the virus's spike glycoprotein, which is the protein that the body's immune system uses to recognise host cells [5]. Additionally, many immunocompromised people might not be completely protected following vaccination [6]. The Omicron variant, which replaced older variants, has become the dominant variant globally. Currently, Omicron HV.1 and JN.1 subvariants have quickly replaced the early Omicron BA.2, BA.5, BA.2.75. and XBB.1 subvariants. Although infections caused by the Omicron variant have decreased in severity, they still pose a significant threat to public health. The virus's mutations can weaken vaccines, weakening the protective barrier. Researchers and vaccine developers are constantly monitoring these changes and adapting strategies to address emerging variants [7–9].

Therefore, there is an urgent need to develop a targeted, effective medication for the SARS-CoV-2 infection. To achieve this purpose, a number of strategies could be used, including the inhibition of enzymes that are essential to SARS-CoV-2's life cycle, such as the main protease (Mpro) (nirmatrelvir/ritonavir and lopinavir/ritonavir), RNA-dependent RNA polymerase (remdesivir, favipiravir, and molnupiravir), papain-like protease (disulfiram), helicase (ivermectin), and Nsp15 endoribonuclease NendoU (glisoxepide and idarubicin) [1–3]. Drug repurposing strategy was used to find effective drugs through virtual screening of various approved and investigational drug libraries, such as drug bank, FDA-approved drugs, etc. [4–6]. This approach has more benefits than the conventional drug discovery process, including a lower failure rate, a quicker drug development process, and lower costs [10].

Several therapeutic molecules of diverse clinical uses were approved to treat the COVID-19 patients as hydroxychloroquine, and chloroquine (antimalarial drugs), azithromycin (antibiotics), ritonavir/lopinavir, nirmatrelvir/ritonavir, favipiravir, remdesivir, and molnupiravir (antivirals), ivermectin (antiparasitic), dexamethasone (corticosteroids), tocilizumab, and sarilumab (monoclonal antibodies), baricitinib (immunomodulators), losartan (antihypertensive) and interferons (IFN) [11–17].

2. Rationale and design

Morphy and Rankovic [18] stated that multi-target designed or directed ligands MTDLs are drugs that simultaneously interact with many targets to manipulate multifactorial disorders like Alzheimer's disease, cancer, and infectious diseases. This approach has many benefits, including increased efficacy, fewer side effects, better bioavailability, and a lower chance of developing drug resistance [19–21].

The objective of this work is to identify an inhibitor of RNA-dependent RNA polymerase (RdRp), the Nsp15 of SARS-CoV-2, and the main protease (Mpro) of COVID-19 by applying the MTDLs, and drug repurposing strategies using various computer-aided drug design techniques such as ligand-based pharmacophore modelling, virtual screening, molecular docking, and molecular dynamic simulation. This is intended to prevent a lack of efficacy due to viral mutation escape.

The primary target for the development of antiviral drugs is the main coronavirus protease (MPro), sometimes referred to as 3C-like protease (3CLpro, nsp5), which is essential for virus replication and regulation of the host cell response. It is a dimer, and each monomer contains two regions: an N-terminal catalytic region and a C-terminal area. The two large polyproteins, pp1a and pp1ab, are cleaved into mature non-structural proteins (nsps) [12]. The primary protease inhibitor, nirmatrelvir/ritonavir, was authorized by the WHO for use in patients with non-severe COVID-19 [13].

In the life cycle of coronaviruses and other RNA viruses, RNA-dependent RNA polymerase (RdRp, nsp12) is a crucial enzyme. It controls the transcription and replication of the RNA genome during infection. To perform its tasks, RdRp requires accessory factors like nsp7 and nsp8. Its structure and functionality are conserved by viruses with RNA genomes from various families. Additionally, it has no human equivalent, making it a prime candidate for the creation of new antiviral drugs [3, 12, 14].

For patients with non-severe COVID-19, the WHO has approved the nucleotide analogues molnupiravir and remdesivir as SARS-CoV-2 RdRp inhibitors. Both are prodrugs. In vivo, remdesivir changes into its active triphosphate form. Beta-D-N4-hydroxycytidine, however, is the active form of molnupiravir [13, 14].

Only the Nidovirales contain SARS-CoV-2 endoribonuclease (nsp15/NendoU), which is regarded as a genetic marker for these viruses. It produces 2′–3′ cyclic compounds by cleaving RNA at the 3′ position of uridylates. It prevents the synthesis of IFN-β and is connected to the coronavirus retinoblastoma tumor suppressor protein. Therefore, its suppression is thought to be essential to the SARS-CoV-2 life cycle [9, 15–17].

Pharmacophore-based virtual screening is a commonly applied technique in drug discovery. This process involves generation of a 3D pharmacophore models based on active ligands which can be used in screening virtual libraries of molecules to select/optimise the lead compounds34 to optimize lead compounds [22].

Computer-aided virtual screening is a rapid, efficient, and low-cost method used in modern medicinal chemistry for discovering novel lead compounds. It allows researchers to quickly find active compounds from huge, small-molecule libraries, improving the speed and efficiency of experimental determination. This tool is particularly useful for the discovery and optimization of anti-SARS-CoV-2 lead compounds and shortening the development cycle [23].

Therefore, a variety of *in silico* methods were used to accomplish this study's objectives, including ligand-based pharmacophore and virtual screening to identify novel molecules based on their distinctive features and molecular dynamics studies to assess the stability of the protein-ligand complex under various environmental conditions.

3. Materials and methods

3.1. Pharmacophore model

3.1.1. Generation of the pharmacophore model

The PharmaGIST webserver (http://bioinfo3d.cs.tau.ac.il/PharmaGist/php.php) was used to generate the pharmacophore model since it is capable of quickly and accurately identifying pharmacophores while considering the flexibility of the ligands. Since the process is fully automated, employing the online interface is easy and intuitive [24].

The training set of native ligands of chosen target proteins (pdb codes: 6LU7, 6WXC, and 7BV2) (https://www.rcsb.org/), which were then extracted and combined in Discovery Studio Visualizer (Dassault Systems BIOVIA, Discovery Studio Visualizer, v17.2.0.16349, San Diego: Dassault Systems, (2016) into mol2 format files. A deterministic algorithm is used by the open-source website PharmaGist to find the overlapping possible pharmacophoric sites between the set of ligands [24]. Following an analysis of the data, the pharmacophore with the greatest alignment score was chosen for additional research. The chemical similarity between the acquired pharmacophoric features and their ligands in each dataset was determined using the molecular overlay module of Discovery Studio Visualizer. It uses a fingerprint-based method to quantify and estimate the similarity between the pharmacophores, reporting the overlap on a scale of 0 to 1.

3.1.2. Pharmacophore based virtual screening

The best pharmacophore model obtained from PharmaGist was used as a constraint to screen against the ZINC Drug Database using ZincPharmer (http://zincpharmer.csb.pitt.edu) [25]. ZINCPharmer uses the open-source Pharmer software to enable the interactive search of ZINC Drug Database conformations in just a few minutes, if not seconds.

3.2. Molecular docking

3.2.1. Protein structures retrieval

The crystal structures of COVID-19 main protease (PDB ID: 6lu7, Resolution: 2.16 A), SARS-CoV-2 Nsp15 (PDB ID: 6wxc, Resolution: 1.85 A) [14], and RdRp (RNA-dependent RNA polymerase) (PDB ID: 7BV2, Resolution: 2.50 A) were downloaded in PDB format from the PDB database (https://www.rcsb.org/).

3.2.2. Binding site prediction

Binding site residues were anticipated through a literature survey for SARS-CoV-2 main protease [26], SARS-CoV-2 Nsp15 [17], and SARS-CoV-2 RdRp (RNA-dependent RNA polymerase) [27].

3.2.3. Preparation of ligand library for docking

The 1331 hits from the ZINC Drug Database's pharmacophore ligand-based screening were loaded into PyRx version 0.8 (http://www.sourceforge.net) [28] using the program's built-in Open Babel tool version 2.4.0 [29] and then subjected to energy minimization. The uff geometry optimization force field was used to reduce the ligand energies, with the optimization algorithm set to conjugate gradients at 200 total steps. Then, using Autodock tools, the energy-minimized ligands were changed into the PDBQT form that was suited for docking.

3.2.4. Molecular docking

The graphical user interface of PyRx allows users to perform virtual screening. Both the RMSD scores and the binding affinities of each ligand can be evaluated. AutoDock 4 and AutoDockVina, two docking software programs, imply the Lamarckian Genetic Algorithm and the Empirical Free Energy Scoring Function. The protein and ligand molecules were imported into PyRx and converted to the docking ready PDBQT format using Autodock tools. The AutoDock Vina tools were then used to do the docking operation on PyRx. The grid center was set to the following coordinates: x 3.3477, y 11.8096, z 65.9519 for the SARS-CoV-2 main protease; x 64.1537, y -69.5576, z 30.3641 for the SARS-CoV-2 Nsp15; and x 95.5712, y 97.2218, z 101.8072 for the SARS-CoV-2 RdRp.

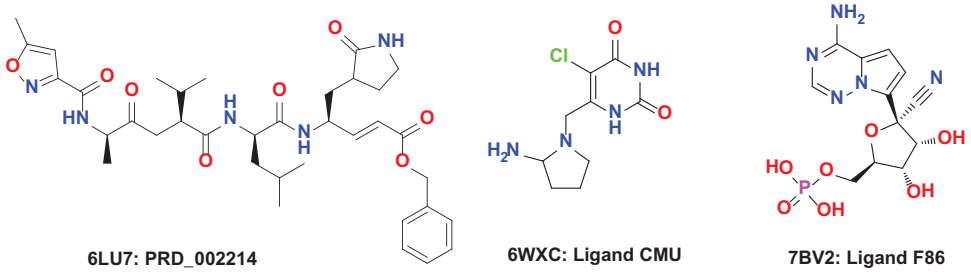

Fig. 1. The co-crystallized ligands of the target proteins.

3.3. ADMET properties determination

The SwissADME server (http://www.swissadme.ch/index.php) was used to predict the physicochemical properties of the glisoxepide (Zn 00537804), which was identified as the best ligand to bind to the three chosen targets among the docked molecules, as well as its corresponding ADMET parameters, pharmacokinetic properties, drug-like nature, and medicinal chemistry friendliness using its SMILES as obtained from the PubChem database (www.pubchem.ncbi.nlm.nih.gov) [30]. Additionally, ProTox-II (tox.charite.de) was used to calculate its potential toxicity features [31].

3.4. Molecular dynamics simulation

The molecular dynamics simulation analysis carried out through the iMODS server (http://imods.chaconlab.org) by normal mode analysis was used to assess the conformational stability of the interactions between our targets (6lu7, 6wxc, and 7BV2) and glisoxepide (Zn 00537804), which was revealed as the best ligand bind to the three selected targets among the docked molecules (NMA). iMODS is an efficient molecular dynamics simulation engine that may be used to analyze the structural dynamics of protein complexes quickly, easily, effectively, and intuitively. It makes predictions about the protein-ligand interactions' elastic network, deformability, mobility profiles, eigenvalues, variance, and covariance map [32].

4. Results and discussion

In this study, the researchers aimed to develop a multi-target pharmacophore-based virtual screening agent against COVID-19. The selected targets for this agent were RNA-dependent RNA polymerase (RdRp), COVID-19 main protease (Mpro), and SARS-CoV-2 Nsp15. The following is a theoretical discussion contributing to the results obtained in the study.

4.1. Theoretical discussion

The development of a multi-target pharmacophore-based virtual screening agent presents a promising approach for identifying potential drugs against COVID-19. By targeting multiple proteins involved in the viral life cycle, the agent aims to enhance effectiveness and reduce the likelihood of viral mutation escape.

The selection of RdRp, Mpro, and Nsp15 as the target proteins is based on their crucial roles in the replication and regulation of SARS-CoV-2. RdRp is responsible for viral RNA synthesis, making it an attractive target for antiviral drug development [3, 12, 14]. Mpro plays a vital role in viral replication by cleaving polyproteins into functional proteins, making it a key target for inhibition [12, 13]. Nsp15, an endoribonuclease, is involved in viral RNA processing and has been identified as a potential target for antiviral interventions [9, 15–17].

The use of virtual screening and molecular docking techniques allowed for the identification of glisoxepide as a potential candidate with high binding affinity to RdRp, Mpro, and Nsp15. Glisoxepide demonstrated favorable binding free energies for all three target proteins, indicating strong interactions within their active sites.

The subsequent MD simulations provided insights into the dynamic behavior and stability of the glisoxepide-protein complexes. The observation of good dynamics and stability suggests that glisoxepide has the potential to maintain its binding and inhibitory effects on the target proteins over time.

It is important to note that the results presented in this study are based on computational approaches and *in silico* investigations. Further experimental research is necessary to validate the efficacy and safety of glisoxepide as a potential treatment for SARS-CoV-2.

In summary, the development of a multi-target pharmacophore-based virtual screening agent provides a promising strategy for identifying potential drugs against COVID-19. The theoretical findings

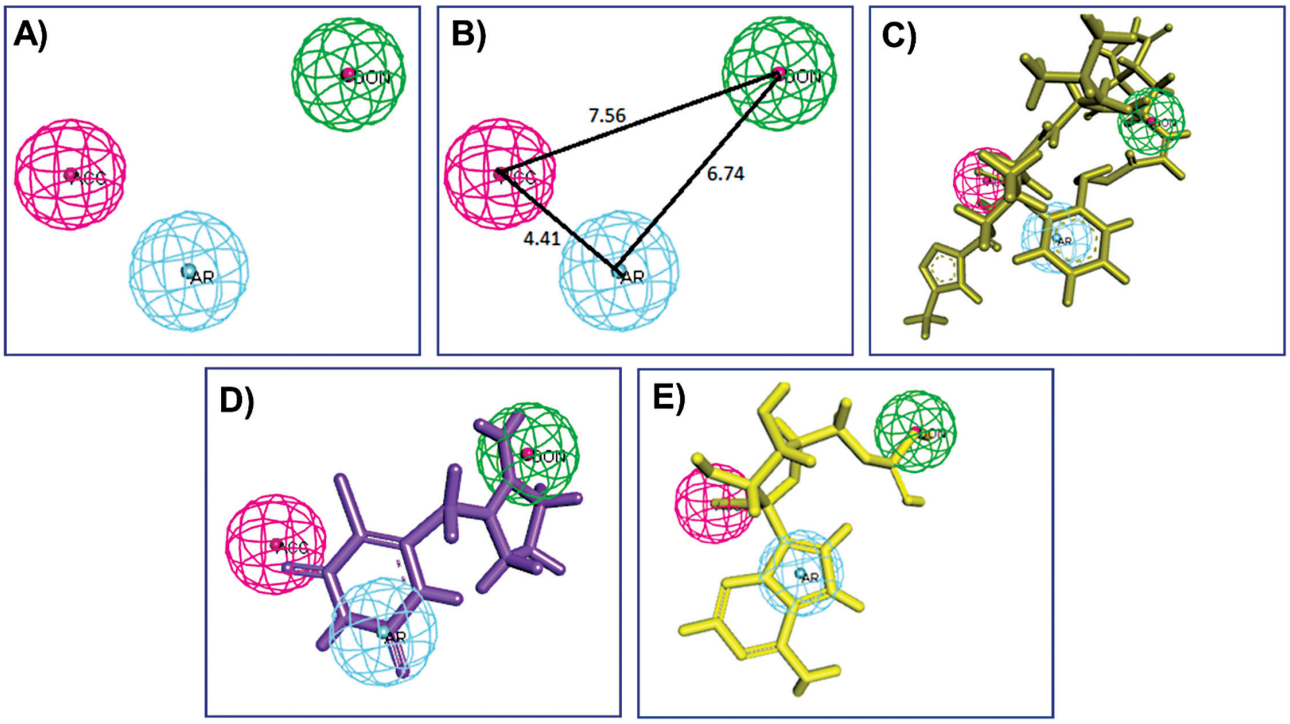

Fig. 2. Details of the best pharmacophore model (a, b) and mapping of test ligands to the pharmacophore model (c, d, e). (a) Spatial disposition of the pharmacophoric features. Hydrogen bond acceptor (ACC, purple), hydrogen bond donor (DON, green), ring aromatic (AR, blue). (b) Distances between feature centers. (c) Mapping of 6lu7; (d) Mapping of 6WXC; (e) Mapping of 7BV2 to the candidate pharmacophore.

suggest that glisoxepide exhibits strong binding affinity and favorable dynamics within the active sites of RdRp, Mpro, and Nsp15. These results warrant further experimental investigations to assess the therapeutic potential of glisoxepide and its suitability for clinical development.

4.2. Pharmacophore model

The researchers employed the PharmaGIST web server to develop a multi-target pharmacophore for RdRp, Mpro, and Nsp15. Pharmacophore modeling is an essential technique in drug design that identifies the critical features necessary for ligand-receptor interaction [33]. By using the native ligands of the chosen targets, the researchers constructed a pharmacophore model that represents the common features required for binding to these proteins. The accuracy of the pharmacophore model depends on the quality of the training set and the selection of features used to define the pharmacophoric points. If the training set is not representative or the chosen features do not adequately capture the essential interactions, the model may have limited predictive power [34].

4.2.1. Generation of the pharmacophore model

The data produced by PharmaGIST for test ligands was analyzed, and the pharmacophore with the highest alignment score was selected. In this model, an aromatic ring, a hydrogen bond acceptor, and a hydrogen bond donor were found to have three pharmacophoric properties. The model features' spatial arrangement was specified in Fig. 2(a), and Fig. 2(b) indicated the distances between feature centers. Select inhibitors' mapping to the pharmacophore model is shown in Fig. 2(c–e). (Fig. 2).

4.2.2. Pharmacophore-based virtual screening

The ZINCPharmer server output uses a Jmol-based molecular viewer to display the distinctive pharmacophore features inside the aligned input ligands. The aromatic ring, hydrogen bond donor, and hydrogen bond acceptor pharmacophore characteristics were represented in purple, grey, and orange mesh, respectively, while the aligned input ligands were shown as sticks (Fig. 3).

This pharmacophore was used as a query to screen the Zinc Drug Database, consisting of around 20432 compounds, using ZINCPharmer.

Table 1. Results of the docking study of glisoxepide into 6LU7, 6WXC, and 7BV2.

			Type of interactions				
			Hydrogen bonding			Hydrophobic	
Target (pdb)	Ligand	ΔG_b[a]	HBs[b]	Ligand[c]	AA[d]	Length[e]	AA[d]
6LU7	glisoxepide	−6.8	4	NH	THR24	2.38	MET49, LEU142
				O	SER46	2.33	
				CO	ASN142	2.22	
				CO	GLY143	2.95	
6WXC	glisoxepide	−6.2	5	NH	THR167	2.11	LYS90, LYS205, LYS277
				NH	ARG199	2.66	
				CO	ASN200	2.06	
				O	ARG207	2.85	
				CO	TYR279	2.55	
7BV2	glisoxepide	−7.8	4	CO	SER682	2.95	MET54, ASP623, VAL557, ALA688
				OH	ASP684	2.39	
				CO	ALA688	2.25	
				CO	THR687	2.63	

[a]Binding free energy (kcal/mol); [b]HBs, number of hydrogen bonds; [c]Atoms in the ligand involved in H-bonds; [d]Amino acids in proteins involved in H-bonds/hydrophobic interactions; [e]length in angstrom (Å).

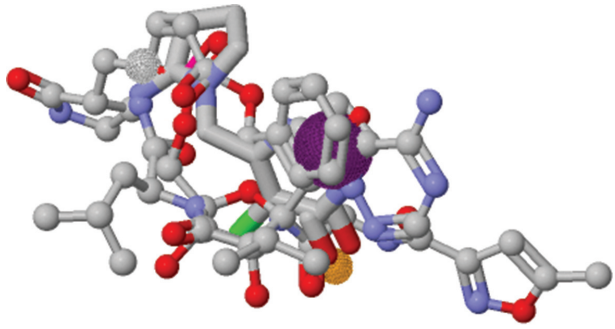

Fig. 3. Three-dimensional structural alignment display of the test ligands, shows the three points with consensus pharmacophore features. The regions of the consensus hydrogen bond acceptor are shown in orange mesh, the region of the consensus hydrogen bond donor is shown in grey mesh, and the region of the consensus aromatic ring is shown in purple mesh.

Pharmacophore-based screening yielded 1331 hits, which were further docked into the binding sites of selected proteins (6lu7, 6wxc, and 7bv2).

4.3. Molecular docking

The ZINC Drug Database's 1331 hits from the pharmacophore-based screening were retrieved as a single SDF file and loaded onto PyRx version 0.8. The goal of this process was to identify the docked molecule that would have the highest binding affinity for the three chosen targets. Based on binding affinity, each hit was scored. Bound native ligands of each target were employed as controls to verify the screening and redocking protocols. For the molecules 6lu7, 6wxc, and 7bv2, respectively, the binding affinities ranged from −3.2 to −7.5 kcal/mol, 20.9 to −7.5 kcal/mol, and 1.5 to −8.4 kcal/mol (Tables S1, S2, and S3). When a compound's binding energy is less than 6.0 kcal/mol, it is expected that it will be active against protein [35]. Glisoxepide (Zn 00537804), among the docked molecules, was identified as the best ligand for binding to the three chosen targets after docking findings were evaluated. The interactions and binding affinities of glisoxepide with our targets were demonstrated in (Table 1). According to the findings, glisoxepide binds to 6LU7, 6WXC, and 7BV2 with binding free energies of −6.8, −6.2, and −7.8 kcal/mol, respectively. With THR24, SER46, ASN142, GLY143 in 6LU7, THR167, ARG199, ASN200, ARG207, TYR279 in 6WXC, and SER682, ASP684, ALA688, and THR687 in 7BV2, it interacted via establishing hydrogen bonds. Additionally, it created hydrophobic connections with MET49, LEU142 in 6LU7, LYS90, LYS205, and LYS277 in 6WXC, and MET54, ASP623, VAL557, and ALA688 in 7BV2 (Fig. 4, Table 1).

The significance of the interactions between glisoxepide and the target proteins can be attributed to the potential inhibitory effects of glisoxepide on their biological functions. As a multi-target agent against the COVID-19 virus, glisoxepide has the potential to disrupt the activities of RNA-dependent RNA polymerase (RdRp), COVID-19 main protease (Mpro), and SARS-CoV-2 Nsp15.

The interactions between glisoxepide and the target proteins may involve various molecular forces, such as hydrogen bonding, and hydrophobic interactions. These interactions play a crucial role in stabilizing the binding between glisoxepide and the target proteins, thereby potentially inhibiting their enzymatic activities.

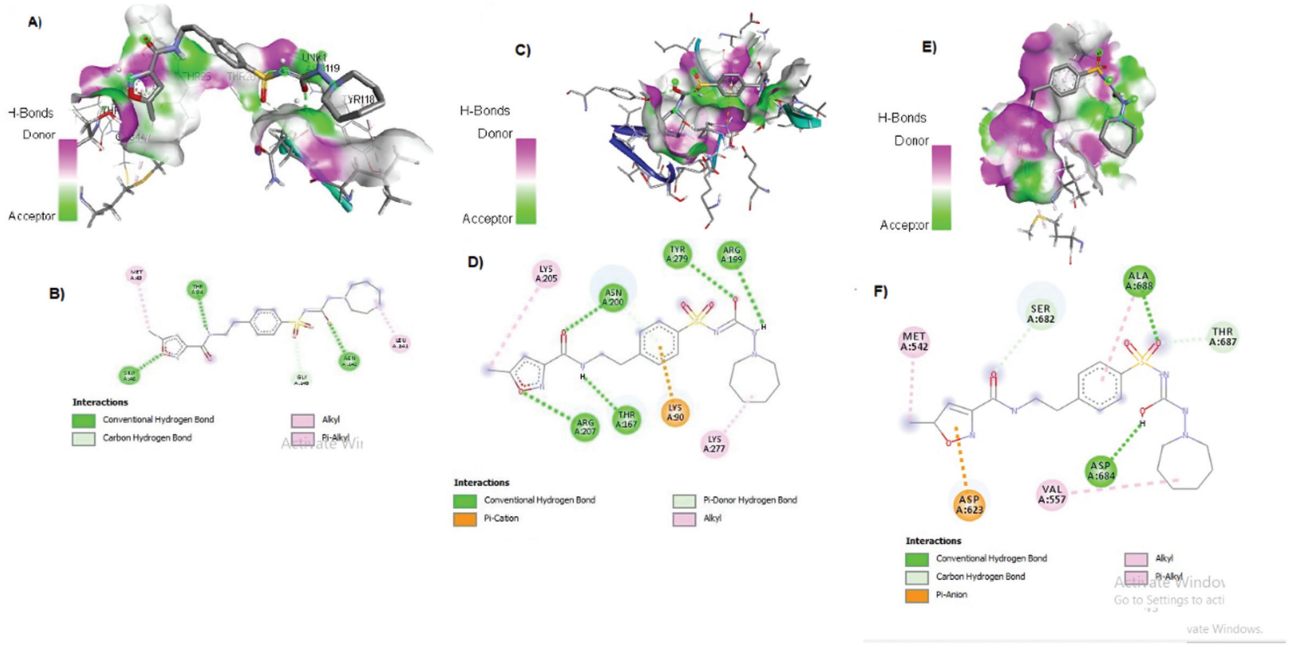

Fig. 4. Binding mode and interactions of glisoxepide into (A) the 3D binding mode of glisoxepide into the active site of the 6LU7 receptor, shown as a hydrogen-bond surface; (B) the 2D binding mode of glisoxepide into 6LU7; (C) the 3D binding mode of glisoxepide into the active site of the 6WXC receptor, shown as a hydrogen-bond surface; (D) the 2D binding mode of glisoxepide into the 6WXC receptor; (E) the 3D binding mode of glisoxepide into the active site of the 7BV2 receptor, shown as a hydrogen-bond surface; (F) the 2D binding mode of glisoxepide into the 7BV2 receptor.

Further experimental research is necessary to validate the effectiveness of glisoxepide as a potential treatment for SARS-CoV-2. However, based on the docking results and the observed interactions, glisoxepide shows promise as a candidate compound for further evaluation and development as an antiviral agent against COVID-19.

4.4. ADMET properties determination

The SwissADME website (http://www.swissadme.ch/) was used to estimate the ADMET characteristics of glisoxepide. The results are presented in Tables 2 to 4. It has a TPSA of 142.02Å^2, a molecular weight of 449.52 g/mol, and 31 heavy atoms. It had a Consensus log Po/W of 3.00, which is p 5. Glisoxepide's predicted water solubility was based on three distinct models: ESOL, Ali, and SILICOS-IT. According to Sorkun *et al.* [36], log S values between 0 and 2 indicate solubility, while values between 2 and 4 suggest mild solubility, and values less than 4 indicate insolubility. Its average log S value was −3.59, indicating that it is only slightly soluble (Table 2). Additionally, it demonstrated poor intestine absorption, as evidenced by its affinity for glycoprotein, log Kp values less than 2.5 cm/s, and good skin penetration potential [37]. The finding that glisoxepide could pass the blood-brain barrier, however, suggested that more research be done into its toxicity. Additionally, the fact that it was unable to block CYP2C19 suggested that it could be able to halt the metabolism of several therapeutic pharmaceuticals, including analgesic, sedative, anticonvulsant, and anti-ulcer medications (Table 3) [38]. Additionally, it was unable to inhibit the enzymes CYP1A2 and CYP2D6, which suggests that it could inhibit liver metabolism and stop the metabolism of antihypertensitive drugs, beta-blockers, antiarrhythmic drugs, and antidepressants, whereas it was able to inhibit the enzymes CYP2C9 and CYP3A4, which indicates the potency of stopping the oxidation of steroids, fatty acids, and xenobiotics Additionally, Fig. 5 and Table 4 exhibit the glisoxepide theoretical drug-likeness data. It was anticipated that the glisoxepide would not be orally accessible because its radar plot at the polarity and flexibility points fell below the acceptable range (Fig. 5). Glisoxepide, however, complied with all drug-likeness rules, except for Veber and Egan rules since its TPSA is greater than 140 and 131.6, respectively (Table 4) [25]. This was determined by the appraiser of the respective drug's likeness using various rule-based filters, including the Lipinski, Ghose, Veber, Egan, and Muegge filters.

Table 2. Physicochemical properties of glisoxepide.

Properties	Glisoxepide
Molecular weight (g/mol)	449.52
Number of heavy atoms	31
Number of arom. heavy atoms	11
Fraction Csp3	0.45
Number of rotatable bonds	10
Number of H-bond acceptors	7
Number of H-bond donors	3
Molar Refractivity	116.58
TPSA	142.02 Å^2
Lipophilicity	
Log Po/w (iLOGP)	2.17
Log Po/w (XLOGP3)	3.50
Log Po/w (WLOGP)	3.07
Log Po/w (MLOGP)	3.13
Log Po/w (SILICOS-IT)	3.15
Consensus Log Po/w	3.00
Water solubility	
Log S (ESOL)	−3.36
Log S (Ali)	−3.97
Log S (SILICOS-IT)	−3.44

Table 3. Pharmacokinetics properties of glisoxepide.

Properties	Glisoxepide
GI absorption	Low
BBB permeant	No
P-gp substrate	Yes
CYP1A2 inhibitor	No
CYP2C19 inhibitor	No
CYP2C9 inhibitor	Yes
CYP2D6 inhibitor	No
CYP3A4 inhibitor	Yes
Log K_p (skin permeation)	−6.98 cm/s

GI = gastro-intestinal absorption, BBB = blood-brain barrier, P-gp = permeability glycoprotein.

Table 4. Predictive drug-likeness of glisoxepide.

Properties	Glisoxepide
Lipinski	Yes; 0 violation
Ghose	Yes
Veber	No; 1 violation: TPSA > 140
Egan	No; 1 violation: TPSA > 131.6
Muegge	Yes
Bioavailability Score	0.55

glisoxepide's virtual toxicological evaluation showed that it is non-toxic due to the fact that its toxic dose was 10000 mg/kg, and it was in class 6 (Table 5) [26].

4.5. Molecular dynamics simulation

It was crucial to study molecular dynamics to evaluate protein-ligand binding, which can be done by comparing protein dynamics in their normal mode. Essential molecular dynamics was also used in this study to analyze a variety of our targets' normal modes to assess their mobility and stability using the iMODS server. We investigated the binding kinetics of the three docked complexes that included glisoxepide with 6LU7, 6WXC, and 7BV2 (Fig. 6). Fig. 6A displayed the 3D interaction models of glisoxepide with the complexes 6LU7, 6WXC, and 7BV2.

The deformity graph showed peaks that correspond to portions of the protein that are deformable; the deformability calculation was based on the individual distortion of each residue; the hinges of the plot correspond to residues with high deformability (Fig. 6B). The B-factor values indicated the relative amplitude of atomic displacements around the equilibrium state and were inferred via NMA to be equivalent to RMS (Fig. 6C). A lower eigenvalue suggested simpler deformation as less energy is required to distort the complex structure, according to the motion stiffness of C atoms computed using the eigenvalue coupled with the confirmed normal mode model. The eigenvalues for glisoxepide with the 6LU7, 6WXC, and 7BV2 complexes were determined to be 1.06661810-4,

Table 5. Oral toxicity prediction results of glisoxepide.

Properties	Glisoxepide
LD50 (mg/kg)	10000
Toxicity Class	6
Hepatotoxicity	Inactive
Carcinogenicity	Inactive
Immunotoxicity	Inactive
Mutagenicity	Inactive
Cytotoxicity	Inactive
Aryl hydrocarbon receptor	Inactive
Androgen receptor	Inactive
Androgen receptor ligand binding domain	Inactive
Aromatase	Inactive
Oestrogen receptor alpha	Inactive
Oestrogen receptor ligand binding domain	Inactive
Peroxisome proliferator activated receptor-c	Inactive
Nuclear factor (erythroid-derived 2)-like 2/ antioxidant responsive element	Inactive
Heat shock factor response element	Inactive
Mitochondrial membrane potential	Inactive
p53	Inactive
ATPase family AAA domain-containing protein 5	Inactive

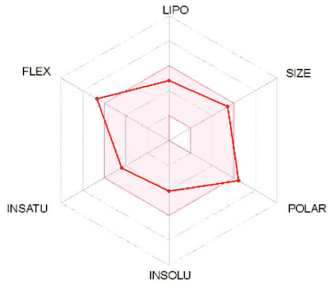

Fig. 5. Suitability for oral administration of glisoxepide. LPO = lipophilicity, POLAR = polarity, INSOLU = solubility, FLEX = flexibility, and INSAT = saturation.

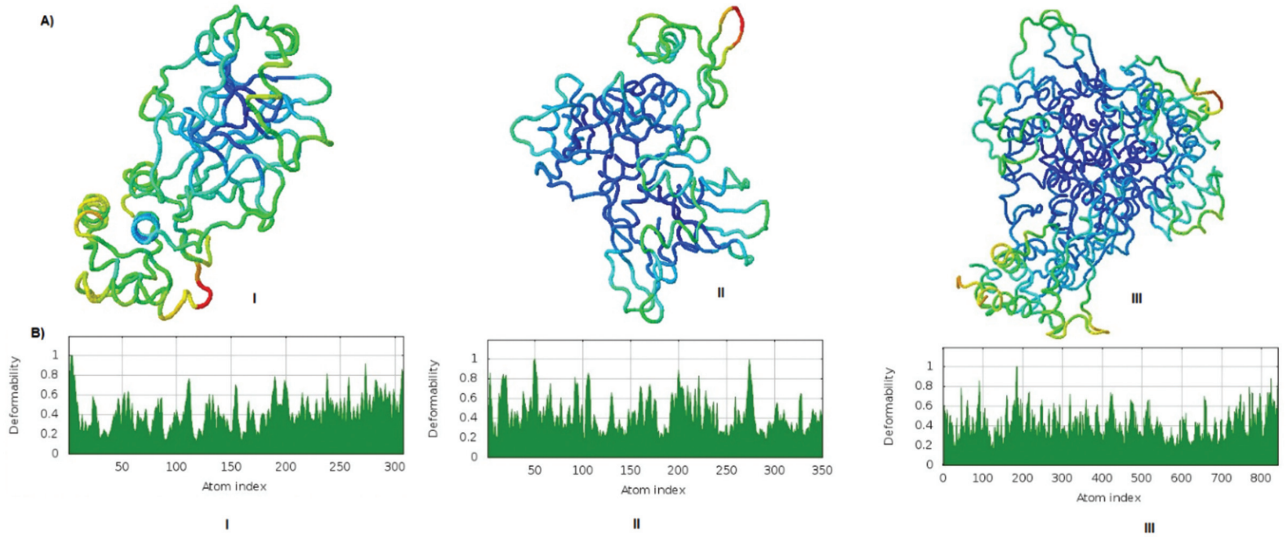

Fig. 6. A and B. Molecular dynamics simulations show (A) NMA mobility and (B) main-chain deformability. The elastic network model of (i) glisoxepide in 6LU7, (ii) glisoxepide in 6WXC, and (iii) glisoxepide in 7BV2.

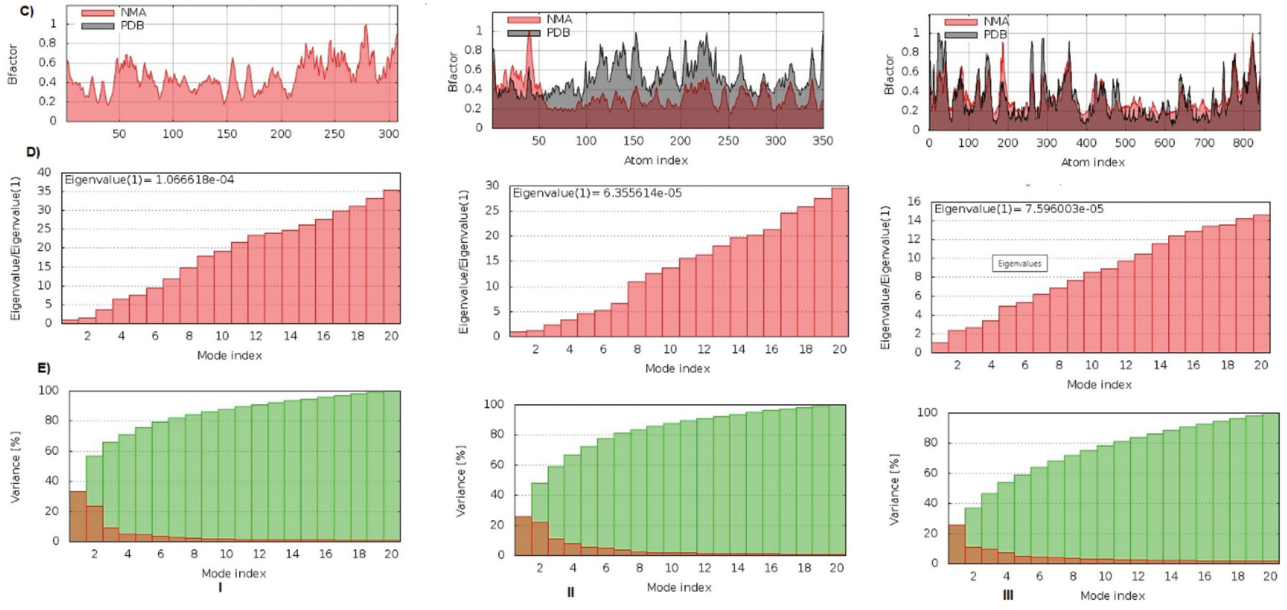

Fig. 6. C, D, and E. (C) experimental B-factor, (D) Eigenvalues, (E) variance associated with each normal mode. The elastic network model of (i) glisoxepide in 6LU7, (ii) glisoxepide in 6WXC, and (iii) glisoxepide in 7BV2.

6.35561410-5, and 7.59600310-5, respectively. These values showed the complexes to be extremely stable (Fig. 6D). The variance plot showed individual variances in red, whereas cumulative variances were in green (Fig. 6E). The covariance matrix demonstrated the connection between pairs of residues, with the correlated, uncorrelated, and anticorrelated pairs of residues being represented by the red, white, and blue colors, respectively (Fig. 6F). Whereas an elastic network map represented the pairings of atoms connected by springs, and each dot in the graph represented a spring between the corresponding pair of atoms. Stronger springs are shown by a darker gray in the graph (Fig. 6G).

Our compounds clearly displayed a good degree of deformability, as demonstrated by the previous molecular dynamics investigation. They also exhibited a moderate eigenvalue, which indicated the possibility of deformation. In contrast to individual variations, the variance map showed a larger level of cumulative variances. A satisfactory result was also obtained with the elastic network map.

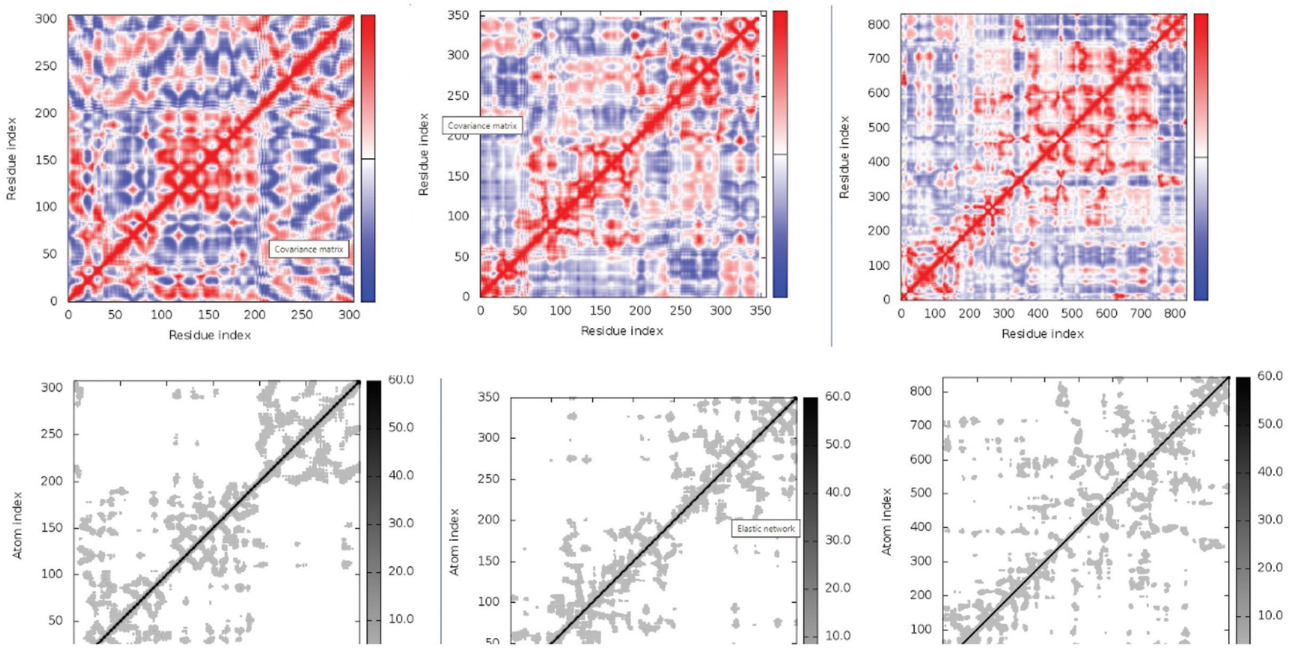

Fig. 6. F and G. (F) Covariance matrix, (G) The elastic network model of (i) glisoxepide in 6LU7, (ii) glisoxepide in 6WXC, and (iii) glisoxepide in 7BV2.

5. Conclusion

In this study researchers developed a multi-target pharmacophore model for SARS-CoV-2, targeting RNA-dependent RNA polymerase, Mpro, and Nsp15. This model aids in screening and identifying potential drug candidates. Ultimately, the goal of this model is to develop effective therapeutics that can effectively combat the virus, minimize viral mutation escape, and enhance the overall efficacy of treatment options for COVID-19.

The pharmacophore-based virtual screening and docking techniques identified 1331 potential hits from the ZINC Drug Database. These hits were then docked to three viral proteins: Mpro, Nsp15, and RdRp. glisoxepide (Zn 00537804) showed the highest binding scores, indicating its potential as a therapeutic candidate. A molecular dynamics simulation study confirmed its favorable dynamics and stability, indicating its sustained inhibitory effect on the targeted viral proteins. This study highlights the value of a drug repurposing strategy that accelerates drug development by utilising compounds with known safety profiles and pharmaceutical properties.

The findings of this study provide a solid foundation for further experimental research to validate the efficacy of glisoxepide and explore its potential as a therapeutic agent for COVID-19. Experimental studies are necessary to confirm the *in silico* findings and assess the safety and effectiveness of glisoxepide in vivo.

The novelty and significance of the study's findings lie in the development of a multi-target pharmacophore model, the identification of glisoxepide as a potential therapeutic candidate, and the demonstration of its stability within the active sites of key viral proteins. These findings contribute to the growing body of knowledge on multi-target drug design for COVID-19 and provide valuable insights for future research and drug development efforts in combating the disease.

Supplementary data

Supplementary material includes copies of docking results of glisoxepide with 6LU7, 6WXC, and 7BV2 **(Tables S1, S2, and S3).**

Acknowledgments

The authors would like to thank the Deanship of Scientific Research at Shaqra University, Beni-Suef University and Deraya University.

Conflict of interest

Authors declared that there is no conflict of interest and have approved the article.

Statements and declarations

We declare that all information in this manuscript is true and correct to the best of our knowledge and belief.

References

1. M. Imran, *et al.*, "Discovery, development, and patent trends on molnupiravir: a prospective oral treatment for COVID-19," *Molecules*, vol. 26, p. 5795, 2021.
2. "World Health Organization WHO Therapeutics and COVID-19 LIVING GUIDELINE 10th Edition," *World Heal. Organ.*, p. 128, 2022.
3. A. Chandra, V. Gurjar, I. Qamar, and N. Singh, "Identification of potential inhibitors of SARS-COV-2 Endoribonuclease (EndoU) from FDA approved drugs: a drug repurposing approach to find therapeutics for COVID-19," *J. Biomol. Struct. Dyn.*, vol. 39, pp. 4201–4211, 2021. doi:10.1080/07391102.2020.1775127.
4. B. M. Sahoo, B. V. V. Ravi Kumar, J. Sruti, M. K. Mahapatra, B. K. Banik, and P. Borah, "Drug Repurposing Strategy (DRS): emerging approach to identify potential therapeutics for treatment of novel coronavirus infection," *Front. Mol. Biosci.*, vol. 8, pp. 1–11, 2021. doi:10.3389/fmolb.2021.628144.
5. C. Chakraborty, A. R. Sharma, M. Bhattacharya, G. Agoramoorthy, and S. S. Lee, "The drug repurposing for COVID-19 clinical trials provide very effective therapeutic combinations: lessons learned from major clinical studies," *Front. Pharmacol.*, vol. 12, pp. 1–15, 2021. doi:10.3389/fphar.2021.704205.
6. M. A. Martinez, "Efficacy of repurposed antiviral drugs: lessons from COVID-19." *Drug Discov. Today*, vol. 27, pp. 1954–1960, 2022. doi:10.1016/J.DRUDIS.2022.02.012.
7. X. He, *et al.*, "The receptor binding domain of SARS-CoV-2 omicron subvariants targets Siglec-9 to decrease its immunogenicity by preventing macrophage phagocytosis," *Nat. Immunol.*, 2024. doi:10.1038/s41590-024-01776-2.
8. B. Hu, *et al.*, "Divergent trajectory of replication and intrinsic pathogenicity of SARS-CoV-2 Omicron Post-BA.2/5 Subvariants in the upper and lower respiratory tract," *eBioMedicine*, vol. 99, p. 104916, 2024. doi:10.1016/j.ebiom.2023.104916.
9. N. D. Kushwaha, *et al.*, "A comprehensive review on the global efforts on vaccines and repurposed drugs for combating COVID-19," *Eur. J. Med. Chem.*, vol. 260, p. 115719, 2023. doi:10.1016/j.ejmech.2023.115719.
10. S. Pushpakom, *et al.*, "Drug repurposing: progress, challenges and recommendations," *Nat. Rev. Drug Discov.*, vol. 18, pp. 41–58, 2018. doi:10.1038/nrd.2018.168.
11. S. L. Senanayake, "Overcoming nonstructural protein 15-Nidoviral Uridylate-Specific Endoribonuclease (Nsp15/NendoU) activity of SARS-CoV-2," *Futur. Drug Discov.*, vol. 2, 2020. doi:10.4155/fdd-2020-0012.
12. C. Gil, *et al.*, "COVID-19: drug targets and potential treatments," *J. Med. Chem.*, vol. 63, pp. 12359–12386, 2020. doi:10.1021/acs.jmedchem.0c00606.
13. R. L. Atmar, and N. Finch, "New perspectives on antimicrobial agents: molnupiravir and Nirmatrelvir/Ritonavir for treatment of COVID-19," *Antimicrob. Agents Chemother.*, p. e0240421, 2022. doi:10.1128/aac.02404-21.
14. W. Yin, *et al.*, "Structural basis for inhibition of the RNA-Dependent RNA polymerase from SARS-CoV-2 by Remdesivir," *Science (80-.)*, vol. 368, pp. 1499–1504, 2020. doi:10.1126/science.abc1560.
15. M. Saramago, *et al.*, "The Nsp15 nuclease as a good target to combat SARS-CoV-2: mechanism of action and its inactivation with FDA-approved drugs," *Microorganisms*, vol. 10, 2022. doi:10.3390/microorganisms10020342.
16. S. Mahmud, *et al.*, "Targeting SARS-CoV-2 nonstructural protein 15 Endoribonuclease: an in silico perspective," *Future Virol.*, vol. 16, pp. 467–474, 2021. doi:10.2217/fvl-2020-0233.
17. Y. Kim, *et al.*, "Tipiracil binds to uridine site and inhibits Nsp15 endoribonuclease NendoU from SARS-CoV-2," *Commun. Biol.*, vol. 4, 2021. doi:10.1038/s42003-021-01735-9.
18. R. Morphy, and Z. Rankovic, "Designing multiple ligands – medicinal chemistry strategies and challenges," *Curr. Pharm. Des.*, vol. 15, pp. 587–600, 2009. doi:10.2174/138161209787315594.
19. R. R. Ramsay, M. R. Popovic-Nikolic, K. Nikolic, E. Uliassi, and M. L. Bolognesi, "A perspective on multi-target drug discovery and design for complex diseases," *Clin. Transl. Med.*, vol. 7, 2018. doi:10.1186/s40169-017-0181-2.
20. N. Gupta, P. Pandya, and S. Verma, "Computational predictions for multi-target drug design," *Methods Pharmacol. Toxicol.*, pp. 27–50, 2019. doi:10.1007/7653_2018_26.
21. J. Zhou, *et al.*, "Rational design of multitarget-directed ligands: strategies and emerging paradigms," *J. Med. Chem.*, vol. 62, pp. 8881–8914, 2019. doi:10.1021/acs.jmedchem.9b00017.
22. A. M. Shawky, N. A. Ibrahim, M. A. S. Abourehab, A. N. Abdalla, and A. M. Gouda, "Pharmacophore-based virtual screening, synthesis, biological evaluation, and molecular docking study of novel pyrrolizines bearing Urea/Thiourea moieties with potential cytotoxicity and CDK inhibitory activities," *J. Enzyme Inhib. Med. Chem.*, vol. 36, 2021. doi:10.1080/14756366.2020.1837124.
23. S. Xu, H. Yuan, L. Li, K. Yang, and L. Zhao, "Computational screening of potential bromodomain-containing protein 2 inhibitors for blocking SARS-CoV-2 infection through pharmacophore modeling, molecular docking and molecular dynamics simulation," *Arab. J. Chem.*, vol. 17, p. 105365, 2024. doi:10.1016/j.arabjc.2023.105365.
24. D. Schneidman-Duhovny, O. Dror, Y. Inbar, R. Nussinov, and H. J. Wolfson, "PharmaGist: a webserver for ligand-based pharmacophore detection," *Nucleic Acids Res.*, vol. 36, pp. 223–228, 2008. doi:10.1093/nar/gkn187.
25. D. R. Koes and C. J. Camacho, "ZINCPharmer: pharmacophore search of the ZINC database," *Nucleic. Acids Res.*, vol. 40, 2012. doi:10.1093/nar/gks378.
26. Z. Jin, *et al.*, "Structure of M pro from COVID-19 virus and discovery of its inhibitors," *Nature*, doi:10.1038/s41586-020-2223-y.
27. W. Yin, *et al.*, "Structural basis for inhibition of the SARS-CoV-2 RNA polymerase by Suramin," *Nat. Struct. Mol. Biol.*, vol. 28, pp. 319–325, 2021. doi:10.1038/s41594-021-00570-0.
28. S. Dallakyan and A. J. Olson, "Small-molecule library screening by docking with PyRx," *Methods Mol. Biol.*, vol. 1263, doi:10.1007/978-1-4939-2269-7_19.
29. N. M. O'boyle, M. Banck, C. A. James, C. Morley, T. Vandermeersch, and G. R. Hutchison, *Open Babel: An Open Chemical Toolbox*, 2011.
30. A. Daina, O. Michielin, and V. Zoete, "SwissADME: A free Web tool to evaluate pharmacokinetics, drug-likeness and medicinal chemistry friendliness of small molecules," *Sci. Rep.*, vol. 7, pp. 1–13, 2017. doi:10.1038/srep42717.
31. M. N. Drwal, P. Banerjee, M. Dunkel, M. R. Wettig, and R. Preissner, "ProTox: a web server for the in silico prediction of rodent oral toxicity," *Nucleic Acids Res.*, vol. 42, pp. 53–58, 2014. doi:10.1093/nar/gku401.

32. J. R. López-Blanco, J. I. Aliaga, E. S. Quintana-Ortí, and P. Chacón, “IMODS: internal coordinates normal mode analysis server,” *Nucleic Acids Res.*, vol. 42, 2014. doi:10.1093/nar/gku339.
33. D. Schaller, *et al.*, “Next generation 3D pharmacophore modeling,” *Wiley Interdiscip. Rev. Comput. Mol. Sci.*, vol. 10, pp. 1–20, 2020. doi:10.1002/wcms.1468.
34. D. Giordano, C. Biancaniello, M. A. Argenio, and A. Facchiano, “Drug design by pharmacophore and virtual screening approach,” *Pharmaceuticals*, vol. 15, pp. 1–16, 2022. doi:10.3390/ph15050646.
35. S. Shityakov and C. I.n Förster, “Silico predictive model to determine vector-mediated transport properties for the blood-brain barrier choline transporter,” *Adv. Appl. Bioinforma. Chem.*, vol. 7, pp. 23–36, 2014. doi:10.2147/AABC.S63749.
36. M. C. Sorkun, A. Khetan, and S. Er, “AqSolDB, a curated reference set of aqueous solubility and 2D descriptors for a diverse set of compounds,” *Sci. Data*, vol. 6, pp. 1–8, 2019. doi:10.1038/s41597-019-0151-1.
37. Y. Han, J. Zhang, C. Q. Hu, X. Zhang, B. Ma, and P. I.n Zhang, “Silico ADME and toxicity prediction of ceftazidime and its impurities,” *Front. Pharmacol.*, vol. 10, pp. 1–12, 2019. doi:10.3389/fphar.2019.00434.
38. S. K. Enmozhi, K. Raja, I. Sebastine, and J. Joseph, “Andrographolide as a potential inhibitor of SARS-CoV-2 main protease: an in silico approach,” *J. Biomol. Struct. Dyn.*, vol. 0, pp. 1–7, 2020. doi:10.1080/07391102.2020.1760136.